Polymer
Chemistry

COMMUNICATION

View Article Online
View Journal | View Issue

Cite this: *Polym. Chem.*, 2016, **7**, 2639

Received 13th October 2015,
Accepted 17th March 2016

DOI: 10.1039/c5py01659b

www.rsc.org/polymers

Rapidly-cured isosorbide-based cross-linked polycarbonate elastomers†

Tyler S. Kristufek,‡[a] Samantha L. Kristufek,[a] Lauren A. Link,[a] Andrew C. Weems,[b] Sarosh Khan,[a] Soon-Mi Lim,[a] Alexander T. Lonnecker,[a] Jeffery E. Raymond,[a] Duncan J. Maitland[b] and Karen L. Wooley*[a]

The rapid synthesis of an optically-transparent, flexible elastomer was performed utilizing the naturally-derived source, isosorbide. A novel monomer based on isosorbide (isosorbide dialloc, IDA) was prepared by installing carbonate functionalities along with external olefins for use in thiol–ene click chemistry. Cross-linked networks were created using the commercially-available cross-linker, trimethylolpropane tris(3-mercaptopropionate) (TMPTMP) and resulted in IDA-*co*-TMPTMP, an optically-transparent elastomer. Systematically, IDA-*co*-TMPTMP networks were synthesized using a photoinitiator, a UV cure time of one minute and varied post cure times (0–24 h, 125 mm Hg) at 100 °C to observe effects on mechanical, thermal and surface alterations. The mechanical properties also had limited changes with post cure time, including a modulus at 25 °C of 1.9–2.8 MPa and an elongation of 220–344%. The thermal decomposition temperatures of the networks were consistent, *ca.* 320 °C, while the glass transition temperature remained below room temperature for all samples. A cell viability assay and fluorescence imaging with adherent cells are also reported in this study to show the potential of the material as a biomedical substrate. A degradation study for 60 days resulted in 8.3 ± 3.5% and 97.7 ± 0.3% mass remaining under accelerated (1 M NaOH, 60 °C) and biological conditions (pH 7.4 PBS at 37 °C), respectively. This quickly-synthesized material has the potential to hydrolytically degrade into biologically-benign and environmentally-friendly by-products and may be utilized in renewable plastics and/or bioelastomer applications.

Introduction

The use of safe, natural products is one avenue to introduce sustainability and utility into materials. Specifically, by adopting renewable resources, there is a decrease in the reliance on petrochemicals that are inherently unsustainable in their current state. Considering easily mass produced, inexpensive starting materials from natural products would allow for natural material to begin to rival petrochemicals as a source for monomers.[1–4] Derived from sugars, 1,4:3,6-dianhydrohexitols (*e.g.* isosorbide, isomannide and isoidide), especially isosorbide, have served as attractive renewable starting materials, contributing to a large assortment of bio-based/inspired polymers due to both the rigidity of their fused ring systems and the easily-modifiable dual-hydroxyl functionalities.[5] 1,4:3,6-Dianhydro-D-sorbitol, isosorbide is readily available in a few steps from biomass sources.[6] Mass production of this material has been utilized by Mitsubishi Chemical through the incorporation of isosorbide into what they call “the world’s first high performance bio-based polycarbonatediol.”[7] Isosorbide has also been incorporated into other polycarbonates,[8,9] polymethacrylates,[10–12] polyesters[13–15] and other polymers.[5,16,17]

Although there has been a large amount of industrial and academic research focused on isosorbide-based materials, one area that has had limited exploration utilizing isosorbide is elastomers formed by thiol–ene click chemistry to produce cross-linked networks.[18–21] Specifically, isosorbide was functionalized with allyl ether moieties and subsequently copolymerized with a tri-functional mercaptopropionate. The resulting bio-based elastomers exhibited T_g values ranging −10 to −2 °C and have the potential to hydrolytically degrade through the ester linkages.[18,19,21] One previously-reported strategy to induce degradability is to functionalize hydroxyl groups to create carbonate linkages. This strategy was employed to produce degradable poly(thioether-*co*-carbonate) networks derived from the natural product quinic acid.[22] In contrast to esters, which produce acids upon hydrolysis, carbonates are converted to carbon dioxide and hydroxyl-containing compounds upon degradation.[23,24] By including carbonate link-

---

[a] *Departments of Chemistry, Chemical Engineering and Materials Science & Engineering, Texas A&M University, P.O. Box 30012, College Station, TX 77842, USA. E-mail: wooley@chem.tamu.edu*

[b] *Department of Biomedical Engineering, Biomedical Device Laboratory, Texas A&M University, Texas 77843, USA*

† Electronic supplementary information (ESI) available: The synthesis and characterization of IDA-*co*-TMPTMP. See DOI: 10.1039/c5py01659b

‡ T. S. K. Current address: Department of Chemistry, Carnegie Mellon, Pittsburgh, PA 15213 and Department of Chemical Engineering, University of Pittsburgh, Pittsburgh, PA 15260.

ages at the hydroxyl sites, it is possible to design a material from isosorbide that has the potential to also produce isosorbide as it degrades. The goal of this work is to produce rapidly-photo-cross-linked isosorbide-based elastomers *via* thiol–ene chemistry that also have the potential to hydrolytically break down into their original natural building blocks. These materials can have applications similar to other bioelastomers including scaffolding materials or soft tissue engineering[25] or starch-based biopolymers including renewable plastics.[26]

Herein is described the synthesis of a novel isosorbide-based monomer, isosorbide dialloc, (IDA) (Scheme 1). IDA contains terminal olefins capable of thiol–ene cross-linking *via* radical addition of a thiol across the alkene. Copolymerization of IDA and commercially-available, trimethylolpropane tris(3-mercaptopropionate) (TMPTMP) in the presence of a photoinitiator was achieved by mixing IDA and TMPTMP based on equal molar functional groups and exposing to UV light (365 nm) for 1 minute. Cross-linking was confirmed by consumption of the alkene (1650 cm^{-1}) and thiol (2570 cm^{-1}) groups in both FTIR and Raman spectra. Networks were subjected to a post-cure at an elevated temperature and under reduced pressure (100 °C, 125 mm Hg) for times ranging from 0–24 h. The effect of post-cure time was evaluated by examining the surface chemistry (contact angle, Raman and IR spectroscopy) as well as the thermal (DSC/TGA) and mechanical (DMA and stain-to-failure measurements) properties to understand if the application of heat after the photo-reaction is necessary to give the optimal properties of the synthesized materials.

Results and discussion

The monomer IDA was prepared in one step by functionalizing 1,4:3,6-dianhydro-D-sorbitol, isosorbide, with two alloc functionalities using allyl chloroformate under conditions as described previously (Scheme 1).[22] Briefly, to install the alloc groups *N*,*N*,*N*′,*N*′-tetramethylethylenediamine was added to isosorbide dissolved in dichloromethane and cooled to 0 °C. Allyl chloroformate was added dropwise at 0 °C and the reaction mixture was allowed to warm to room temperature overnight to deliver a purified yield of 86% as a lightly viscous, colourless oil. The synthesis of the monomer was confirmed by ^{1}H NMR, ^{13}C NMR, COSY, ATR-FTIR and ESI-MS (ESI Fig. 1–4†).

Polycarbonates derived from the natural product isosorbide were designed with several attractive features. Isosorbide includes a fused-ring system that is non-toxic and chiral, both of which are beneficial to the final material.[5,27] Functionalizing isosorbide *via* installation of allyl carbonates served two purposes. First, the carbonate functionality allows for potential degradation back to isosorbide and CO_2, resulting in an environmentally/biologically-friendly product. Various carbonate-based co-polymers have been shown to be degradable in other

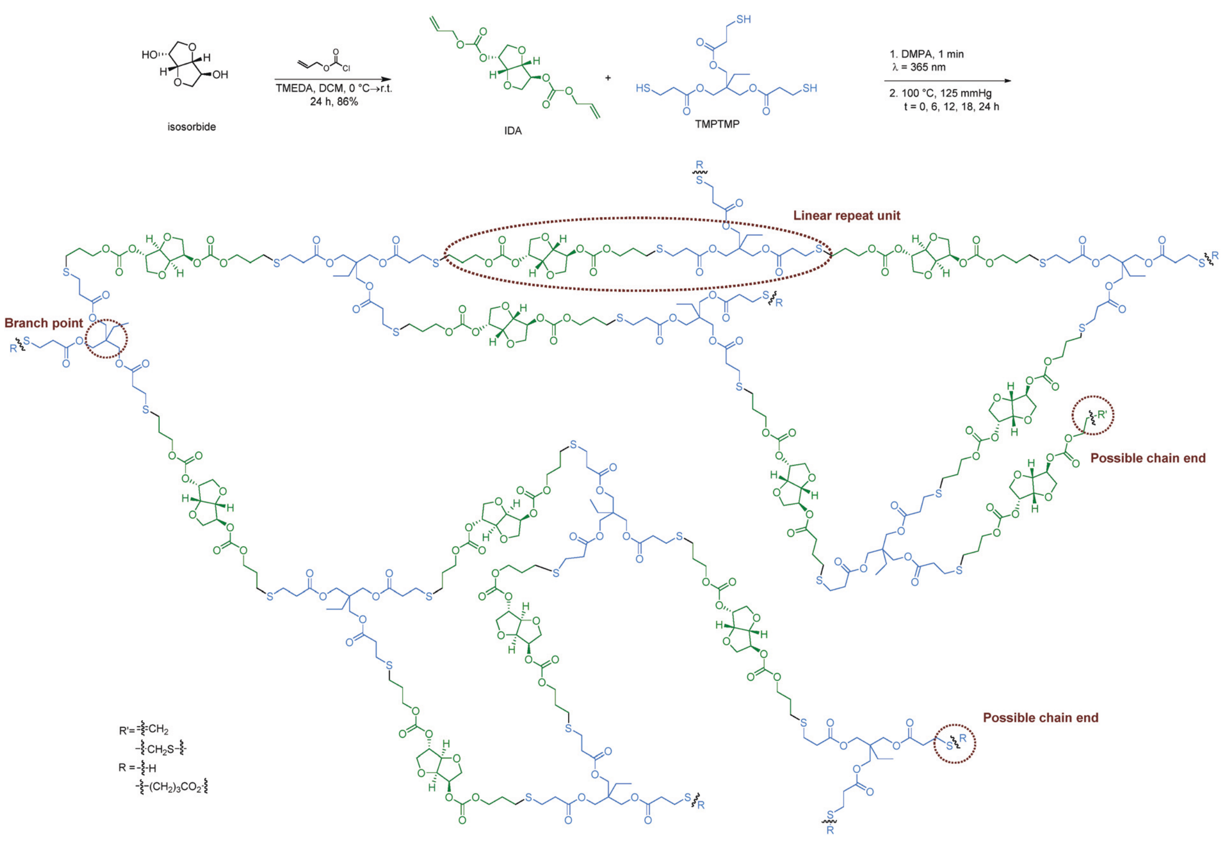

Scheme 1 Synthesis of the monomer IDA and the cross-linked network, IDA-*co*-TMPTMP.

cross-linked networks.[28] Secondly, the alkene was introduced for polymerization and/or cross-linking by thiol–ene click chemistry. Click chemistry has become a widely used, simple, prominent concept in organic synthesis, polymerizations, and materials chemistry due to multiple factors: no/low solvent systems, limited excess material, high efficiency, low catalyst loading under ambient conditions, and insensitivity to the presence of moisture.[29–31] In these studies, focus was upon cross-linked network formation, involving reaction of commercially-available trimethylolpropane tris(3-mercaptopropionate) (TMPTMP) with IDA to afford an optically-transparent, flexible material, IDA-*co*-TMPTMP. Besides the thiol functionalities that were used for cross-linking, TMPTMP also has ester linkages, which may act as other potential degradation sites.[32] With degradation as the intention of these types of materials, TMPTMP has been previously been studied *in vivo* for toxicity and found to be a good candidate for these types of materials.[32] Ester cross-linkers are well known to have flexible and elastomeric properties[33] that, when combined with the rigid structure of IDA, are expected to yield a tough yet ductile material. The cross-linker is trifunctional, so by combining it with the difunctional IDA, three-dimensional cross-linked networks with moderate cross-link density can be achieved.

In all experiments, IDA and TMPTMP were mixed in an equal molar ratio based on functional groups, with variation in the curing conditions. Full reaction of the TMPTMP thiol was observed at 1 minute UV curing (λ = 365 nm) and no post-cure heating. This result displays that at least at the surface level, the network can be synthesized quickly under mild conditions including no solvent and limited catalyst loading (*e.g.* 1 wt%).

Thiol consumption was confirmed by Raman and IR spectroscopies with the disappearance of the thiol bands observed at *ca.* 2570 cm^{-1} in parallel with an apparent increase in alkane functionality (2800–2980 cm^{-1}) (ESI Fig. 4A and B†).

To understand whether post-cure heating would exert effects on multiple properties, such as T_g, decomposition temperature (T_d), elongation and storage modulus of the IDA-*co*-TMPTMP films, the post-cure time at 100 °C under vacuum was altered and tested systematically over the range of 0–24 h. The extent of cross-linking reaction was monitored by IR and Raman spectroscopies (Fig. 4A and B†) by following the alkane growth and thiol disappearance. Static water contact angle measurements were taken at five different points on each film and averaged (ESI Fig. 5†). Slight changes in the contact angle occurred with the addition of a post-cure. From a post-cure time 0 h temperature for the 1 min UV cure until 18 h the water contact angle steadily increased from 72° to 81° followed by a decrease from 18 h to 24 h, where it returned to 72°. The trend might indicate relaxation of the chains upon application of heat to the material which can induce reorder depending on the time and temperature used during the post-cure process.[34] While there was a change in the surface properties overall, the material remained relatively hydrophobic under all tested conditions. Although the reaction was complete on the surface at one minute of UV irradiation, post-cure heating conditions has the potential to enable vaporization of remaining small molecules, vulcanization of any residual thiols[35] and network relaxation.[34]

The surface morphology, thermal and mechanical properties were, therefore, monitored with the addition of a thermal post-cure at elevated temperature and reduced pressure. The T_d of the networks was measured by thermogravimetic analysis (TGA) and remained nearly constant around 320 °C with the addition of a post-cure (Table 1). The T_g of the networks was measured using differential scanning calorimetry (DSC) and reported the average of three runs. The T_g remained below room temperature in the range from 14 to 18 °C for different post-cure times (Table 1). The thermomechanical behaviour of the networks was determined by dynamic mechanical analysis (DMA), run in tension. The storage modulus as a function of temperature of each network is shown in Fig. 1. These traces are indicative of amorphous cross-linked networks. Three regions of the differing mechanical response were observed with changing temperature. At low temperatures, there was a glassy modulus plateau on the order of 1 GPa. The glass transition region is recognized by the drastic decrease in modulus with increasing temperature. Beyond the glass transition region, the rubbery modulus plateau was constant or slightly increasing with increasing temperature and, in accordance with the rubber elasticity theory, is proportional to the cross-link density of the network. The storage modulus at 25 °C increased from 79 to 550 MPa with the application of a post-cure for at least 18 h. This trend is similar to the trend in hydrophobicity determined by contact angle measurements, which could be due to microstructuring and relaxation of the network as more energy is added to the system. With the exception of the sample that received no post-cure, the rubbery modulus of the networks increased with increasing post-cure time, from 5.8 MPa at 6 h to 7.1 MPa at 24 h, showing a slight increase in cross-link density as a result of additional cross-linking reactions occurring, including the vulcanization of residual thiols and the stiffening of the network as a result of matrix relaxation. The reduction in rubbery modulus from 6.5 MPa at 0 h to 5.8 MPa at 6 h under post-cure conditions is not unusual and may be due to entanglement relaxation. Using the theory of rubber elasticity, the cross-link density (ν_c) defined as the number of moles of elastically effective network chains per cubic centimeter of sample can be calculated with the following equation:

$$\nu_c = \frac{\varepsilon'}{3RT} \tag{1}$$

Table 1 Observed thermal properties of IDA-*co*-TMPTMP networks

Time (h)	T_d (°C)	T_g (°C)
0	317	16.5 ± 0.2
6	320	18.4 ± 0.6
12	322	15.8 ± 0.1
18	322	14.1 ± 0.5
24	322	14.4 ± 0.2

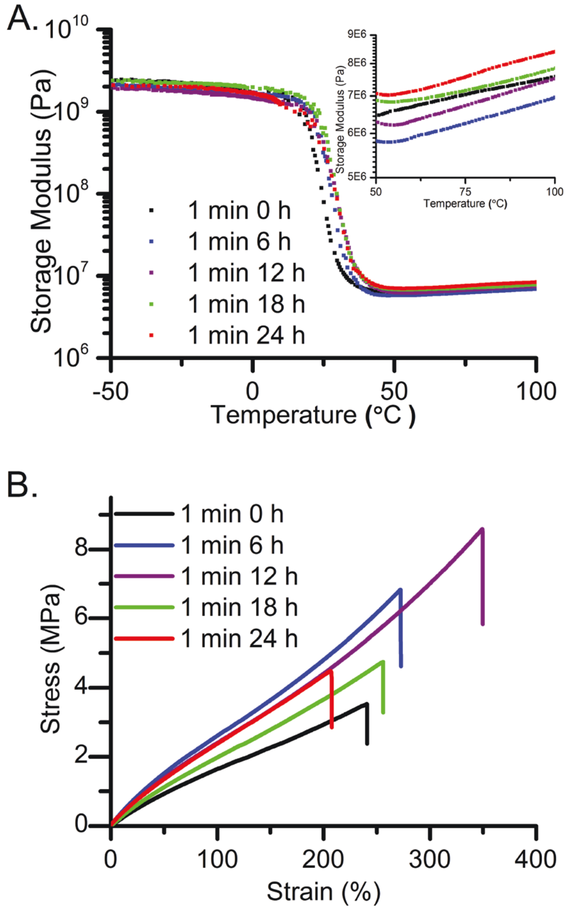

Fig. 1 A. Storage modulus as a function of increasing series with inset zoomed in on the rubbery modulus. B. Representative stain-to-failure curves of IDA-*co*-TMPTMP.

where R is the gas constant, T is the temperature and ε' is the rubbery modulus at 50 °C.[36] Values (Table 2) can be compared to the ideal cross-linked network density of 1.98×10^{-3} mol cm^{-3}. The difference between the theoretical and calculated ν_c is characteristic of a network with incomplete conversion of all functional groups. The cross-link density can be used to calculate the molecular weight between cross-links defined as total sample weight that contains one mole of elastically effective network chains (M_c) using the following equation:

$$M_c = \frac{\rho}{\nu_c} \tag{2}$$

where ρ is the density of the film.[36] The density was measured to be 1.2 g cm^{-3} and the theoretical M_c was calculated to be 606 g mol^{-1}. The measured values are *ca.* 2.5× greater than the calculated values indicative of a non-ideal cross-linked network. The values have limited changes with the application of heat showing the networks are cross-linked to the fullest extent permitted by the chemical structure within the confined space of the reaction.

To further characterize the mechanical properties of IDA-*co*-TMPTMP, ASTM type V dog-bone samples were prepared, by laser cutting sheets of the material, and subjected to strain-to-failure measurements (five of each sample species); representative curves are shown in Fig. 1. The average % elongation, tensile strengths and moduli are shown in Table 2. Consistent with thermal, surfacial and other mechanical data, there were limited changes in the stain-to-failure properties. The modulus increased slightly from 1.9 to 2.8 MPa with the addition of 6 h post-cure, but beyond 6 h, changes were negligible. The % elongation at break ranged from 220–340% and showed no significant change with the addition of a post-cure. The ultimate tensile strength ranged from 3.7–7.8 MPa and was maximized at 12 h post-cure.

Degradation study

With the goal of rapidly UV-cured materials, the bulk materials were subjected to a degradation study under both accelerated and biological conditions. Pellets were formed by casting a mixture of IDA and TMPTMP into moulds and cured then removed from the moulds and cured on the other side (1 min irradiation each side). In the accelerated study, pellets were initially massed dry then submerged into a solution of 1 M NaOH (2.0 mL). Each solution with a pellet was heated to 60 °C with 120 rpm stirring. After two days, the samples were removed from solution, washed with DI water and blotted dry with a Kimwipe. The mass was measured to obtain the wet mass (x_{wet}). The pellets were then dried at 100 °C under vacuum for 2 h. The dry pellets were massed again followed by submersion into a fresh solution of 1 M NaOH and heated to 60 °C. This process was repeated for 60 days. After being submerged in solution, the pellets were translucent (Fig. 2, bottom, left), but after drying, the pellets returned to being transparent (Fig. 2, bottom, right). Degradation occurred at a closely linear trend for the duration of the study. On day 60,

Table 2 Thermal and mechanical properties of various thermally cured IDA-*co*-TMPTMP networks

Time (h)	Storage modulus[a] (MPa)	E_r[b] (MPa)	Modulus (MPa)	Elongation at break (%)	Tensile strength (MPa)	Toughness (MJ m^{-3})	ν_c (mol cm^{-3})	M_c (g mol^{-1})
0	79	6.5	1.9 ± 0.2	250 ± 40	3.7 ± 0.5	4.9 ± 0.5	8.06×10^{-4}	1488
6	280	5.8	2.8 ± 0.2	280 ± 50	6.6 ± 1.0	9.5 ± 3.0	7.20×10^{-4}	1668
12	430	6.2	2.4 ± 0.2	340 ± 50	7.8 ± 1.0	13.4 ± 3.6	7.69×10^{-4}	1560
18	550	6.9	2.5 ± 0.4	260 ± 40	4.6 ± 1.3	7.2 ± 1.9	8.56×10^{-4}	1402
24	350	7.1	2.8 ± 0.2	220 ± 30	4.6 ± 0.7	5.3 ± 0.2	8.81×10^{-4}	1362

[a] Storage modulus measured by DMA at 25 °C. [b] Rubbery modulus measured at 50 °C.

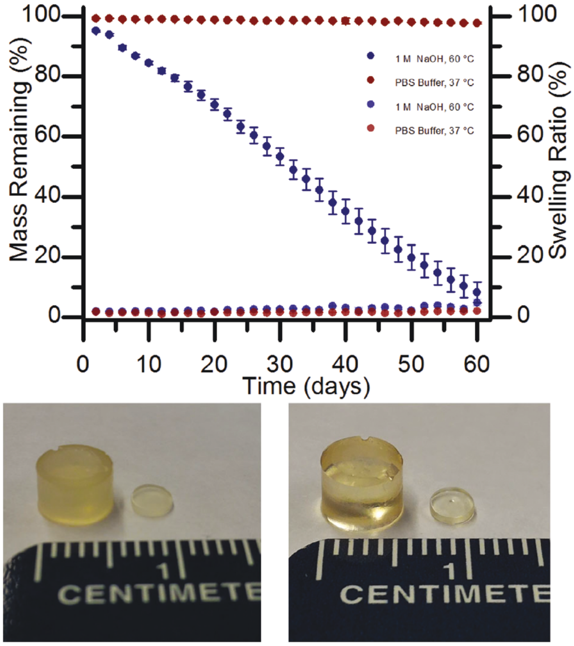

Fig. 2 Degradation study in NaOH, 60 °C (blue) and PBS buffet, pH = 7.4, 37 °C (red). Samples from the degradation study before drying (bottom, left) and after drying (bottom, right).

8.3 ± 3.5% mass remained. The swelling ratio (SR) was calculated using the following equation:

$$\mathrm{SR} = \frac{x_{\mathrm{wet}} - x_{\mathrm{dry}}}{x_{\mathrm{dry}}} \times 100\% \qquad (3)$$

where x_{wet} and x_{dry} are the mass of the wet (after blotting) and dry (after vacuum) materials, respectively. This material had limited swelling over the length of the study with a slight increase in swelling with time (Fig. 2) and a swelling ratio of 4.9 ± 1.1 on day 60. The linear decrease in degradation of the mass with time while maintaining the shape (Fig. 2, bottom) suggests surface erosion of the polymer networks.

Under biological conditions, PBS buffer at 37 °C and pH = 7.4, three pellets were submerged for the same duration as the accelerated study, and were found to show 97.7 ± 0.3% mass remaining on day 60. Under these biological conditions, the swelling ratio increased slightly over time and was 2.1 ± 0.3% on day 60. IDA-*co*-TMPTMP will degrade under biological conditions, but at a slower rate when compared to the accelerated basic conditions.

Cell viability and fluorescence microscopy

IDA-*co*-TMPTMP was tested for the potential for biomedical application by monitoring stable attachment and cytoskeletal development from adherent preosteoblast (MC3T3) cells. Cells were fixed with 2% paraformaldehyde and co-stained with phalloidin-Alexa488 to visualize actin in cytoskeleton and with anti-vinculin and anti-mouse-Alexa647 antibodies to visualize focal adhesions. Cytoskeleton and focal adhesions are dynamic structures and sensitive to the substrate on which the cells reside. Stained cells were imaged with a laser scanning confocal microscope (Olympus FV 1000) with 10× objective. Fluorescence images of cells on the IDA-*co*-TMPTMP-coated glass bottom dishes showed matured cytoskeleton (green) and focal adhesions (red), as observed from cells on a glass surface (Fig. 3), therefore, it is clear that the newly-developed material has potential to be used as a biomedical substance. The cytotoxicity of IDA-*co*-TMPTMP was evaluated against MC3T3 E1 mouse preosteoblast cells, however, IC_{50} values of the copolymers could not be determined because high cell-viabilities were observed.

Conclusions

Overall, a novel cross-linked network system was synthesized using a naturally-derived monomer, isosorbide dialloc (IDA)

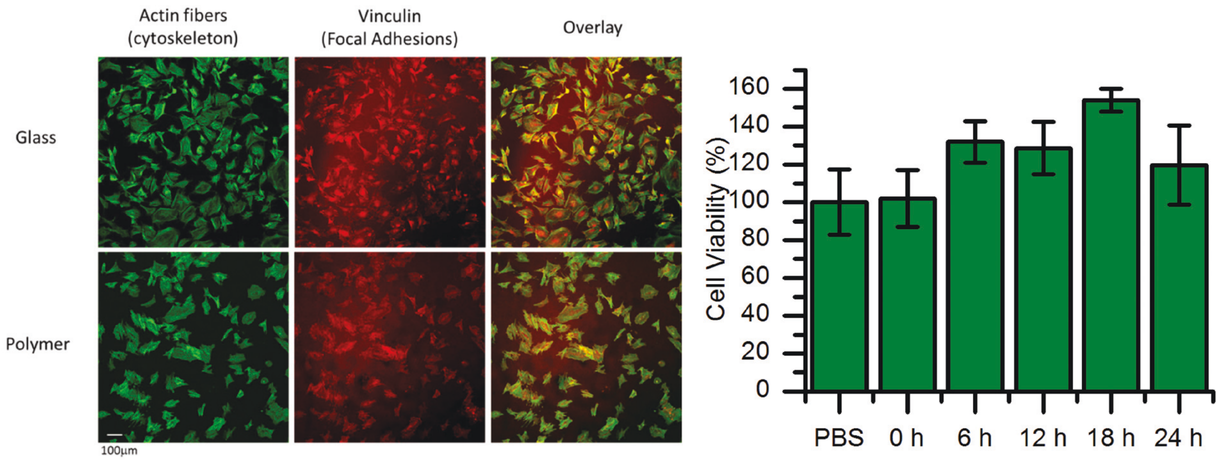

Fig. 3 MC3T3 cells on IDA-*co*-TMPTMP-coated glass bottom dishes (left). Viability of MC3T3 E1 mouse preosteoblast cells of IDA-*co*-TMPTMP polymer at timed intervals with an incubation time of 72 h (right).

and cross-linked with TMPTMP. The optically-transparent, flexible cross-linked networks, IDA-*co*-TMPTMP, were synthesized with environmentally-friendly methods including solvent-free conditions, low catalyst loading and UV irradiation. A study of a constant UV cure time (1 minute) and variation of the thermal curing times led to the conclusion that the material is near its optimal thermal and mechanical properties without requiring post-cure heating. The T_d remained *ca.* 320 °C and the T_g remained below room temperature, in a narrow range. The elastomeric material had a % elongation of 220–340%. The hydrolytic degradation of the material (1 min UV cure, no post cure) was evaluated, and found to afford 8.3 ± 3.5% and 97.7 ± 0.3% mass remaining after 60 days under accelerated aqueous basic and physiological neutral buffer conditions, respectively. MC3T3 cells deposited on IDA-*co*-TMPTMP-coatings showed matured cytoskeletons and focal adhesions as well as high cell-viability. Overall, this novel material has properties that could be useful in biomedical applications or as environmentally-friendly materials.

Conflict of interest

The authors declare no competing financial interest.

Acknowledgements

We gratefully acknowledge financial support from the National Science Foundation (CHE-1057441 and CHE-1410272) and the Welch Foundation (A-0001). Use of the Texas A&M University Laboratory for Synthetic-Biologic Interactions and the Laboratory for Biological Mass Spectrometry, with assistance by Dr Yohannes Rezenom and Vanessa Santiago, are acknowledged. The authors would also like to thank Khoi N. Van for many insightful conversations. The authors thank the Texas A&M University graduate diversity fellowship and the Department of Biomedical Engineering for funding.

References

1 T. Iwata, *Angew. Chem., Int. Ed.*, 2015, **54**, 3210–3215.
2 A. Gandini and T. M. Lacerda, *Prog. Polym. Sci.*, 2015, **48**, 1–39.
3 S. A. Miller, *Polym. Chem.*, 2014, **5**, 3117–3118.
4 S. A. Miller, *ACS Macro Lett.*, 2013, **2**, 550–554.
5 F. Fenouillot, A. Rousseau, G. Colomines, R. Saint-Loup and J. P. Pascault, *Prog. Polym. Sci.*, 2010, **35**, 578–622.
6 M. Rose and R. Palkovits, *ChemSusChem*, 2012, **5**, 167–176.
7 M. M. Bomgardner, *Chem. Eng. News*, 2015, **93**, 15.
8 S. Chatti, G. Schwarz and H. R. Kricheldorf, *Macromolecules*, 2006, **39**, 9064–9070.
9 M. Yokoe, K. Aoi and M. Okada, *J. Polym. Sci., Part A: Polym. Chem.*, 2003, **41**, 2312–2321.
10 J. J. Gallagher, M. A. Hillmyer and T. M. Reineke, *ACS Sustainable Chem. Eng.*, 2015, **3**, 662–667.
11 J. M. Sadler, A.-P. T. Nguyen, F. R. Toulan, J. P. Szabo, G. R. Palmese, C. Scheck, S. Lutgen and J. J. La Scala, *J. Mater. Chem.*, 2013, **1**, 12579–12586.
12 J. J. Gallagher, M. A. Hillmyer and T. M. Reineke, *Macromolecules*, 2014, **47**, 498–505.
13 D. Juais, A. F. Naves, C. Li, R. A. Gross and L. H. Catalani, *Macromolecules*, 2010, **43**, 10315–10319.
14 W. C. Shearouse, L. M. Lillie, T. M. Reineke and W. B. Tolman, *ACS Macro Lett.*, 2015, **4**, 284–288.
15 H. Kang, X. Li, J. Xue, L. Zhang, L. Liu, R. Xu and B. Guo, *RSC Adv.*, 2014, **4**, 19462–19471.
16 M. Okada and K. Aoi, *Curr. Trends Polym. Sci.*, 2002, **7**, 57–70.
17 M. Z. Oulame, F. Pion, S. Allauddin, K. V. S. N. Raju, P.-H. Ducrot and F. Allais, *Eur. Polym. J.*, 2015, **63**, 186–193.
18 C. Lorenzini, A. Haider, I.-K. Kang, M. Sangermano, S. Abbad-Andalloussi, P.-E. Mazeran, J. Lalevée, E. Renard, V. Langlois and D.-L. Versace, *Biomacromolecules*, 2015, **16**, 683–694.
19 R. A. Ortiz, A. Y. R. Martinez and A. E. G. Valdez, *J. Biobased Mater. Bioenergy*, 2012, **6**, 36–41.
20 C. Lorenzini, D. L. Versace, C. Gaillet, C. Lorthioir, S. Boileau, E. Renard and V. Langlois, *Polymer*, 2014, **55**, 4432–4440.
21 T. Modjinou, D.-L. Versace, S. Abbad-Andallousi, N. Bousserrhine, J. Babinot, V. Langlois and E. Renard, *ACS Sustainable Chem. Eng.*, 2015, **3**, 1094–1100.
22 L. A. Link, A. T. Lonnecker, K. Hearon, C. A. Maher, J. E. Raymond and K. L. Wooley, *ACS Appl. Mater. Interfaces*, 2014, **6**, 17370–17375.
23 T. Artham and M. Doble, *Macromol. Biosci.*, 2008, **8**, 14–24.
24 A.-C. Albertsson and M. Eklund, *J. Appl. Polym. Sci.*, 1995, **57**, 87–103.
25 Q. Y. Liu, L. Jiang, R. Shi and L. Q. Zhang, *Prog. Polym. Sci.*, 2012, **37**, 715–765.
26 J. Lörcks, *Polym. Degrad. Stab.*, 1998, **59**, 245–249.
27 Q. Lin, J. Pasatta and T. E. Long, *J. Polym. Sci., Part A: Polym. Chem.*, 2003, **41**, 2512–2520.
28 M. Yokoe, K. Aoi and M. Okada, *J. Appl. Polym. Sci.*, 2005, **98**, 1679–1687.
29 A. Dondoni, *Angew. Chem., Int. Ed.*, 2008, **47**, 8995–8997.
30 H. C. Kolb, M. G. Finn and K. B. Sharpless, *Angew. Chem., Int. Ed.*, 2001, **40**, 2004–2021.
31 K. L. Killops, L. M. Campos and C. J. Hawker, *J. Am. Chem. Soc.*, 2008, **130**, 5062–5064.
32 A. E. Rydholm, C. N. Bowman and K. S. Anseth, *Biomaterials*, 2005, **26**, 4495–4506.
33 S. E. Kasprzak, B. Martin, T. Raj and K. Gall, *Polymer*, 2009, **50**, 5549–5558.
34 J. Shin, S. Nazarenko and C. E. Hoyle, *Macromolecules*, 2008, **41**, 6741–6746.
35 P. M. Imbesi, J. E. Raymond, B. S. Tucker and K. L. Wooley, *J. Mater. Chem.*, 2012, **22**, 19462–19473.
36 L. W. Hill, *Prog. Org. Coat.*, 1997, **31**, 235–243.